Avrupa Bilim ve Teknoloji Dergisi
Özel Sayı 40, S. 88-93, Eylül 2022

Araştırma Makalesi

www.ejosat.com ISSN:2148-2683

European Journal of Science and Technology
Special Issue 40, pp. 88-93, September 2022

Research Article

Effect of Deposition Time on Hardness and Corrosion Properties of Electroless Nickel-Boron Coatings

Yaren Sarp[1*], İbrahim Usta [2], Sezer Tan [3], Hasan Algül [4], Mehmet Uysal [5], Ahmet Alp [6]

[1*] Sakarya University, Metallurgical and Materials Engineering, Sakarya, Turkey, (ORCID: 0000-0003-3043-3643), yarensarp@hotmail.com
[2] Sakarya University of Applied Sciences, Metallurgical and Materials Engineering, Sakarya, Turkey, (ORCID: 0000-0001-7557-9617), b16.ibrahim@gmail.com
[3] Sakarya University, Metallurgical and Materials Engineering, Sakarya, Turkey, (ORCID: 0000-0002-1265-6897), sezertan@sakarya.edu.tr
[4] Sakarya University, Metallurgical and Materials Engineering, Sakarya, Turkey, (ORCID: 0000-0002-4348-8865), halgul@sakarya.edu.tr
[5]Sakarya University, Metallurgical and Materials Engineering, Sakarya, Turkey, (ORCID: 0000-0002-9396-7450), mehmetu@sakarya.edu.tr
[6]Sakarya University, Metallurgical and Materials Engineering, Sakarya, Turkey, (ORCID: 0000-0002-6164-4729), alp@sakarya.edu.tr

(1st International Conference on Innovative Academic Studies ICIAS 2022, September 10-13, 2022)

(**DOI:** 10.31590/ejosat.1173924)

ATIF/REFERENCE: Sarp Y., Usta, I., Tan, S., Algül H., Uysal M., Alp A., (2022). Effect of Deposition Time on Hardness and Corrosion Properties of Electroless Nickel-Boron Coatings. Avrupa Bilim ve Teknoloji Dergisi, (40), 88-93.

Abstract

Electroless nickel-based coatings are an excellent method to improve the surface properties of materials such as wear, hardness and corrosion. On the other hand, aluminum alloys are used in many applications" due to their properties such as cheapness and lightness. In addition to these good properties of aluminum alloys, their poor surface properties are limited in some usage areas in the industry. In this study, electroless nickel-boron (Ni-B) coatings were applied to the aluminum surface to improve the surface properties of the aluminum alloys (6xxxx). In this study, the effect of deposition time (30, 60, 90 min.) on the hardness and corrosion properties of Ni-B coatings was investigated. Scanning electron microscopy (SEM) was used to study the surface morphology, and X-ray diffractometry (XRD) was used to examine the phase structure. According to the SEM analysis results, it was observed as a result of the studies that the morphology of the Ni-B coating changed from nodular structure to cauliflower-like structure with increasing deposition time. Also, the thickness of the coatings is increased with an increase in the deposition time. According to the study's results, although the highest average hardness value is obtained as 1140 Hv by the highest deposition time of 90 min, the highest corrosion resistance is obtained as 1.969×10^{-3} mpy by the lowest deposition time of 30 min.

Keywords: *Nickel-boron, Hardness, Corrosion, Microstructure, Electroless coating,*

Biriktirme Süresinin Akımsız Nikel-Bor Kaplamaların Sertlik ve Korozyon Özelliklerine Etkisi

Öz

Akımsız nikel esaslı kaplamalar, malzemelerin aşınma, sertlik ve korozyon gibi yüzey özelliklerini iyileştirmek için mükemmel bir yöntemdir. Alüminyum alaşımları ise ucuzluk ve hafiflik gibi özelliklerinden dolayı birçok uygulamada kullanılmaktadır. Alüminyum alaşımlarının bu iyi özelliklerinin yanında, düşük yüzey özellikleri endüstrideki bazı kullanım alanlarını sınırlar. Bu çalışmada, alüminyum alaşımlarının (6xxxx) yüzey özelliklerini iyileştirmek için alüminyum yüzeye akımsız nikel-bor (Ni-B) kaplamalar uygulanmıştır. Kaplama süresinin (30, 60, 90 dk.) Ni-B kaplamaların sertlik ve korozyon özellikleri araştırıldı. Yüzey morfolojisini incelemek için taramalı elektron mikroskobu (SEM) ve faz yapısını incelemek için X-ışını difraktometrisi (XRD) kullanıldı. SEM analiz sonuçlarına göre, Ni-B kaplamanın morfolojisinin artan kaplama süresi ile nodüler yapıdan karnabahar benzeri yapıya dönüştüğü deneysel çalışmalar sonucunda gözlemlenmiştir. Kaplamadaki, en yüksek sertlik değeri 90 dakikalık en yüksek biriktirme süresi ile 1140 Hv olarak elde edilmesine rağmen, en yüksek korozyon direnci 30 dakikalık en düşük biriktirme süresi ile 1.969×10^{-3} mpy olarak elde edilmiştir.

Anahtar Kelimeler: Nikel-Bor, Sertlik, Korozyon, Mikroyapı, Akımsız kaplama,

1. Introduction

Electroless coating is a coating method which reduces metal ions onto the catalytic surface by chemical reduction process without applying an external electric current. Electroless nickel coatings are obtained by reducing nickel ions by the action of reducers on a "conductive and catalytic" substrate immersed in a solution containing nickel salts (Loto, 2016). Nickel, combined with phosphorus or boron released by the reductant, forms a binary alloy. Electroless nickel coatings firstly was announced by Brenner and Riddel in the 1940s. Today, electroless nickel coatings are used in extensive applications such as aerospace, automotive, chemical, and electrical industries because of their solderability and high hardness (Parkinson, 1997). Besides, electroless deposition provides the production of wear-resistant hard coatings without using any special equipments (Krishnaveni, Narayanan, & Seshadri, 2005).

Electroless coatings provide a homogenous surface because of their coating mechanism, so the irregular-shaped surfaces can be coated because the coating occurs at every point of the surface in contact with the coating solution.

Electroless nickel-boron coatings have a higher hardness than that of nickel-phosphorous coatings. The hardness of nickel-boron coatings also increases with the amount of boron included. Another attractive property of Ni-B coatings is their wear resistance, which can be compared with that of hard chromium coating. Also, it is believed that Ni-B coating positively contributes to the corrosion resistance of the surfaces [4].

In this study, Ni-B coating was applied onto the 6XXX series aluminum surface by the electroless coating method at different deposition times. The effect of the deposition time on the surface morphologies, corrosion resistances and harnesses of the aluminum substrates is investigated.

2. Material and Method

In the electroless Ni-B deposition process, 20x20x5 mm 6XXX series aluminum alloy samples were used as substrates. Before the electroless coating process, each sample was firstly sanded with SiC paper, then polished with alumina slurry and cleaned in an acidic solution to remove surface dirt and oil. Before the immersion of the substrates into the coating solutions, the pre-treatment process was applied with tin and palladium solutions. The pre-treatment steps are given in Fig. 1. After pre-treatment, the aluminum substrates were immersed in the electroless coating baths. The electroless coating was carried out in solutions of the same conditions in Table 1 with different deposition times of 30,60 and 90 minutes.

The components used in the electroless coating process, and their functions are given in Table 1. The pH of the electroless Ni-B coatings was kept between 5-6 for all coatings. Nickel (II) sulfate hexahydrate as the nickel source, sodium acetate ($C_2H_3NaO_2$) as the complexing agent, thiourea as the stabilizer (CH_4N_2S) and DMAB ($(CH_3)_2NBH_2$) as the reducing agent was used in the coatings. The surface and cross-sectional morphology of the samples were characterized by scanning electron microscopy (SEM). In order to examine the cross-sectional specimens after deposition, the specimens were cut and mounted in bakelite, and after the sanding and polishing processes, they were examined in SEM.

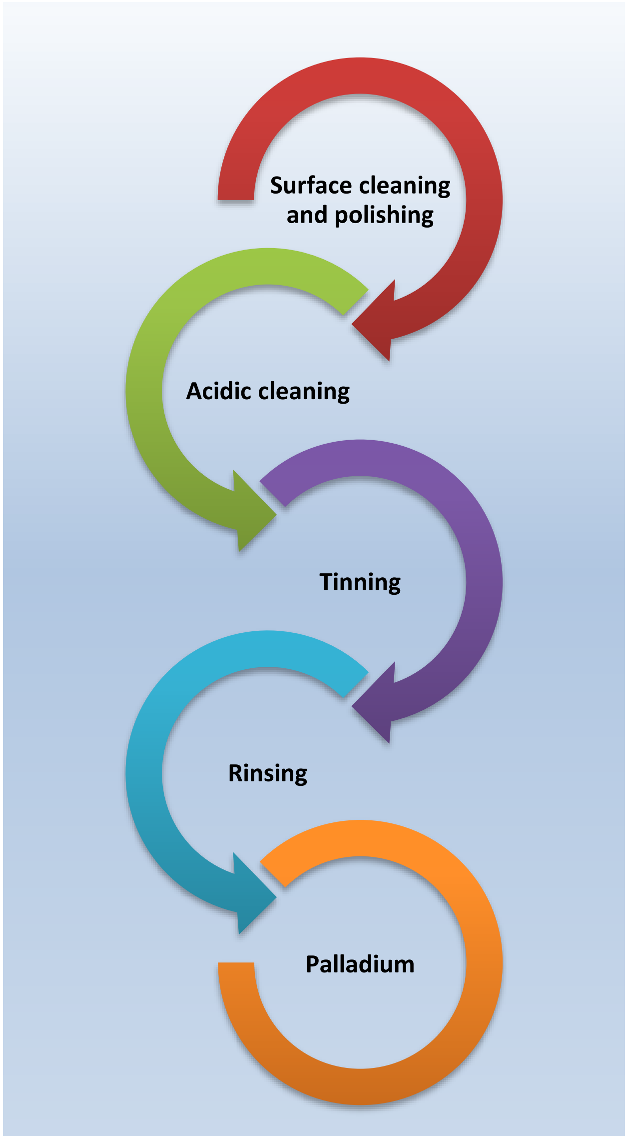

Fig. 1. Electroless sample preparation before coating.

X-ray diffraction (XRD) analyzes of Ni-B alloy coatings were performed with a Rigaku D/max 2200 powder diffraction meter using Cu K-alpha radiation. Hardness tests were carried out with a Vickers Microhardness tester (LEICA VMHTMOT) under the force of 25 gf and indentation time of 10 s.

The potentiodynamic polarization measurements were obtained using Gamry Interface 1000 Potentiostat by scanning the potential from −100 mV to 100 mV at a scan rate of 1 mV s−1. Tafel extrapolation experiments were performed in a three-electrode cell using a saturated calomel electrode (SCE) reference electrode, graphite counter electrode and electroless Ni-B coatings working electrode in 3.5 wt% NaCl solution at room temperature.

Table 1. Bath chemical composition and operating conditions.

Bath chemicals	Chemical Properties	Concentration
Nickel (II) sulfate hexahydrate	*Metallic Ions*	*36 g/L*
Sodium acetate	*Complexing Agent*	*6 g/L*
DMAB	*Reducing Agent*	*10 g/L*
Thiourea	*Stabilizer*	*1 mg/L*
Parameters		
Bath pH	*5-6*	
Deposition time (min.)	*30,60 and 90*	
Bath temperature (°C)	*75-80*	
Stirring Speed (rpm)	*350*	

3. Results and Discussion

The surface morphologies of the coatings at 1000X and 3000x magnifications are presented in Fig. 2. It is clearly seen from figure, the typical cauliflower-like structure became more evident with increasing deposition time. It has been reported that cauliflower-like structure may be formed due to the coaxial growth of grains at the substrate interface induced by the high amount of nucleation sites on the substrate surface (Dominguez-Rios, Torres-Sanchez, & Aguilar-Elguezabal, 2007). The amount of boron in the structure increased with the increasing deposition time, and more nucleation zones were formed. In addition, there are no defects or cracks on the coating surface in all coating conditions.

The cauliflower-like structure is occurred at all deposition times (30, 60, 90 min.). With the increase of the deposition time, the formation and growth of grains increase the reaction rate with the catalytic effect of the core nickel on the substrate and cause the deposition of more boron as well as nickel (Dominguez-Rios et al., 2007). It was observed that the grains got smaller with increasing deposition time and grain boundaries increased. (see Fig. 2. and Fig. 5.)

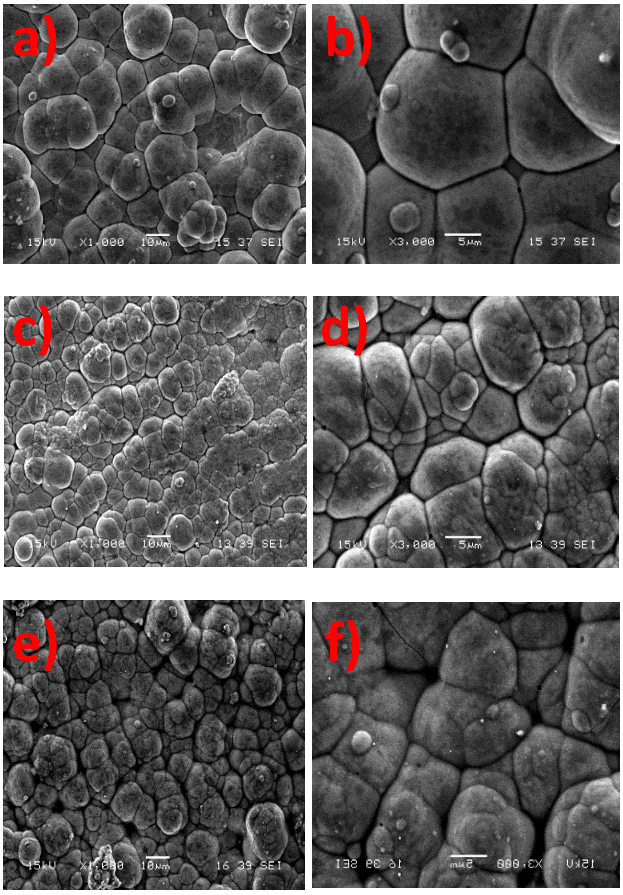

Fig. 2. Different magnification (X1000 and X3000) SEM surface morphology images of different deposition time electroless Ni-B. a-b: 30 min, c-d: 60 min, e-f: 90 min.

Cross-sectional images of Ni-B coatings are presented in Fig. 3. It has been observed that with the increase in deposition time, there is a noticeable increase in the thickness of the coating. In the periods between 30 minutes and 60 minutes, the coating thickness increased slightly. At a deposition time of 90 minutes, there is a significant increase in thickness. As the deposition time increases, the coating thickness increases and a nodular growth occurs columnar on the substrate (Kaya, Gulmez, & Demirkol, 2009). With the increase of the deposition time, the coating thickness increased as a result of the accumulation of nickel ions (Shakoor, Kahraman, Gao, & Wang, 2016). In electroless the thickness of Ni-B coatings is obtained as 10.8, 11.4 and 16.2 µm for different deposition times os 30, 60 and 90 min., respectively.

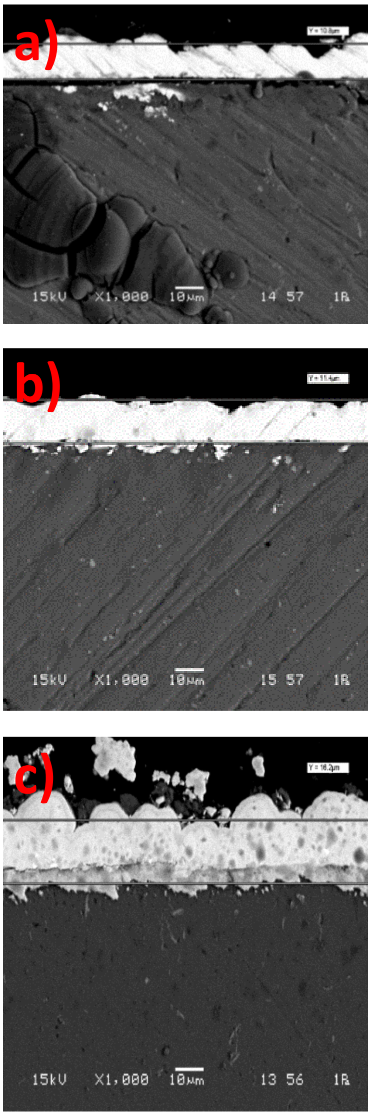

Fig. 3. SEM cross-section images of electroless Ni-B coatings (1000X magnification).

X-ray diffraction (XRD) analyses of Ni-B alloy coatings are produced by the electroless coating method were performed with a Rigaku D/max 2200 powder diffraction meter using Cu K-alpha radiation. The X-ray diffraction patterns of all coatings are shown in Fig. 4. Amorphous/semi-crystalline alloy coatings showed a single Nickel peak at 44° in the (111) plane, as in similar studies (Li et al., 1999). When the peaks at approximately 44° of the coating layers produced with electroless coating are examined, it is clearly seen that the peak intensity becomes sharper with the increase in the the deposition times of the coatings. Also, , the Ni peak (200) at approximately 53° indicates the presence of both amorphous and crystalline structures for the deposition time of 90 min (Tian, Sun, Liu, Jia, & Xiao, 2021).

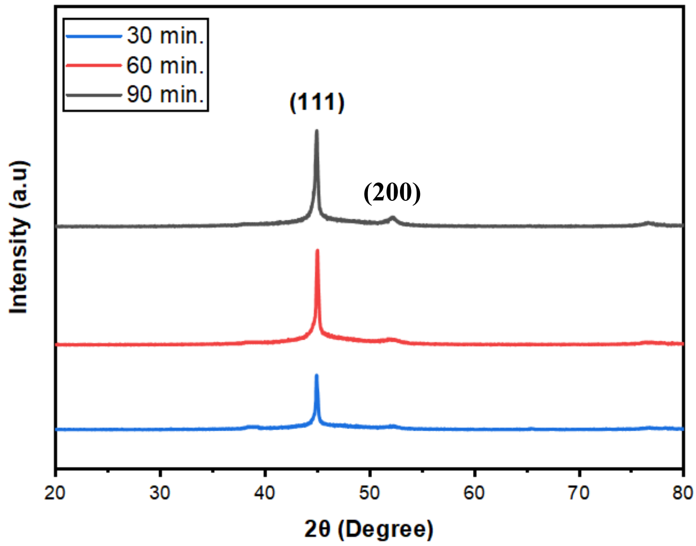

Fig. 4. XRD patterns of coatings produced in different deposition times.

Grain size was calculated using the XRD data with the Scherrer equation (Patterson, 1939) given below.

$$\tau = \frac{K\lambda}{\beta \cos\theta}$$

Table. 2. Boron volume percent of Ni-B coatings according to coating time.

Deposition Time (min.)	B% Content
30	*1.942*
60	*2.489*
90	*4.113*

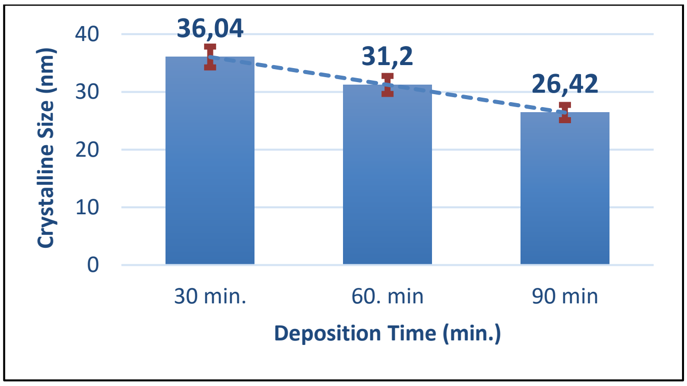

Fig. 5. The crystalline size of the coatings calculated by the Scherrer equation.

The cyrstalline size of the coatings is shown in the Fig. 5. The crystalline size of the coatings is decreased with the increasing deposition time due to nucleation sites increase with the increase in time.

It has been reported that the decreasing in crystalline size highly affects the hardness of the coating (Czagány, Baumli, & Kaptay, 2017). In accordance with the literature, an increase in the hardness value was observed by examining the grain size and the increase in the coating thickness. The hardness values of the coatings were obtained by taking the average of 5 different traces from the cross-sectional surfaces. The hardness values of the coatings are presented in Fig. 6.

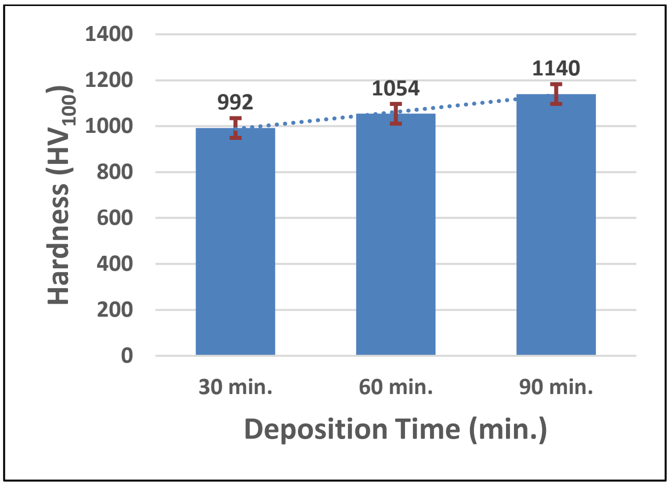

Fig. 6. Hardness values of electroless Ni-B samples (30-60-90 min.)

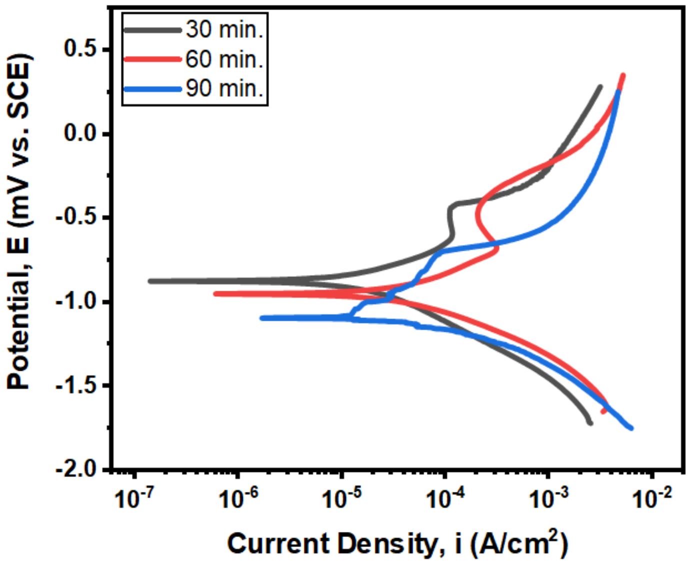

Fig. 7. The Tafel curve at different deposition time of the coating.

Figure 7 shows the potentiodynamic polarization curves of Ni-B coatings coated at different deposition times. Considering the potentiodynamic polarization curves, the sample with the lowest corrosion rate belongs to the Ni-B coating produced in 30 minutes. The corrosion rate is found as 1.98x10-3. This sample is followed by samples of 60 and 90 minutes, respectively. The corrosion rates of these samples are 5.731x10-3 and 6.483x10-3, respectively. The increase in corrosion rates with increasing time is the increasing amount of boron in the coating content. Corrosion resistance is negatively affected by the increase in the amount of boron. With the increase of boron content, passive oxide film formation is prevented and corrosion resistance of the sample decreases (Bekish, Poznyak, Tsybulskaya, & Gaevskaya, 2010).

Table. 3. Corrosion rates obtained from the polarization curves for deposition time.

Deposition Time(min.)	Corrosion Rate (µm/year)
30	*$1.968x10^{-3}$ mpy*
60	*$5.731x10^{-3}$ mpy*
90	*$6.483x10^{-3}$ mpy*

4. Conclusions and Recommendations

Ni-B coatings were successfully produced with electroless at different deposition times (30,60,90 min.). All depositions have a typical cauliflower-like structures. The crystalline size decreased with the increase in deposition time. The thickness of the coatings is increased with increasing of the deposition time. The highest thickness is obtained as 16.2 µm at 90 min. deposition time.

The hardness values of the coatings increased with the increase of the deposition time. The highest hardness value of 1140 HV was reached in 90 minutes.

Considering the potentiodynamic polarization curves, the highest corrosion resistance is achieved in Ni-B coating produced in 30 minutes.

5. Acknowledge

We would like to thank Sakarya University, Metallurgical and Materials Engineering Department for providing the opportunity to carry out our study.

We thank Sakarya University Scientific Research Projects Unit for their support to the project numbered 2018-1-6-37.

We would like to thank TUBITAK for their support to the project numbered 116M998.

References

Bekish, Y. N., Poznyak, S. K., Tsybulskaya, L. S., & Gaevskaya, T. V. (2010). Electrochimica Acta Electrodeposited Ni – B alloy coatings : Structure , corrosion resistance and mechanical properties. *Electrochimica Acta*, 55(7), 2223–2231. Retrieved from https://doi.org/10.1016/j.electacta.2009.11.069

Czagány, M., Baumli, P., & Kaptay, G. (2017). The influence of the phosphorous content and heat treatment on the nano-micro-structure, thickness and micro-hardness of electroless Ni-P coatings on steel. *Applied Surface Science*, 423, 160–169. Retrieved from https://doi.org/10.1016/J.APSUSC.2017.06.168

Dominguez-Rios, C., Torres-Sanchez, R., & Aguilar-Elguezabal, A. (2007). Characterization Of The film Of Ni-B Electroless on Steel S7, Through Optical Microscopy and Scanning Electron Microscopy. *ECS Transactions*, 3(25), 117–122. Retrieved from https://doi.org/10.1149/1.2753246

Kaya, B., Gulmez, T., & Demirkol, M. (2009). Study on the electroless Ni-B nano-composite coatings. *AIP Conference Proceedings*, 1127(September 2014), 62–73. Retrieved from https://doi.org/10.1063/1.3146199

Krishnaveni, K., Narayanan, T. S. N. S., & Seshadri, S. K. (2005). Electroless Ni–B coatings: preparation and evaluation of hardness and wear resistance. *Surface and Coatings Technology*, 190(1), 115–121. Retrieved 8 September 2022 from https://www.academia.edu/1522307/Electroless_Ni_B_coatings_preparation_and_evaluation_of_hardness_and_wear_resistance

Li, H., Li, H., Dai, W. L., Wang, W., Fang, Z., & Deng, J. F. (1999). XPS studies on surface electronic characteristics of Ni–B and Ni–P amorphous alloy and its correlation to their catalytic properties. *Applied Surface Science*, 152(1–2), 25–34. Retrieved from https://doi.org/10.1016/S0169-4332(99)00294-9

Loto, C. A. (2016). Electroless Nickel Plating – A Review. *Silicon 2016 8:2*, 8(2), 177–186. Retrieved 8 September 2022 from https://doi.org/10.1007/S12633-015-9367-7

Parkinson, R. (1997). Properties and Applications of Electroless Nickel. *Nickel Development Institute Publication*, 33. Retrieved from http://www.nickelinstitute.org/TechnicalLiterature/TechnicalSeries/PropertiesandApplicationsofElectrolessNickel_10081_.aspx

Patterson, A. L. (1939). The Scherrer Formula for X-Ray Particle Size Determination. *Physical Review*, 56(10), 978. Retrieved 1 January 2022 from https://doi.org/10.1103/PhysRev.56.978

Shakoor, R. A., Kahraman, R., Gao, W., & Wang, Y. (2016). Synthesis, characterization and applications of electroless Ni-B coatings-A review. *International Journal of Electrochemical Science*, 11(3), 2486–2512.

Tian, S. S., Sun, W. C., Liu, Y. W., Jia, Y. P., & Xiao, Y. (2021). Effect of Na2WO4concentration on the microstructure and corrosion behavior of Ni-W-P ternary alloy coatings. *Materials Research*, 24(4). Retrieved from https://doi.org/10.1590/1980-5373-MR-2020-0580